water

MDPI

Article

Replenishment Impacts on Hydrogeochemistry and Water Quality in the Hutuo River Plain

Ruolin Zhang [1], Baoyun Zhang [2,*], Yuntong Guo [3], Xiangke Kong [4,5], Yasong Li [4,5], Yaci Liu [4,5], Lining Chen [5] and Qiuli Gong [2,*]

1 China Institute of Geo-Environment Monitoring, Beijing 100081, China
2 Institute of Geophysical and Geochemical Exploration, Chinese Academy of Geological Sciences, Langfang 065000, China
3 Network Information Security Laboratory, Heibei GEO University, Shijiazhuang 050031, China
4 Fujian Provincial Key Laboratory of Water Cycling and Eco-Geological Processes, Xiamen 361000, China
5 Institute of Hydrogeology and Environmental Geology, Chinese Academy of Geological Sciences, Shijiazhuang 050061, China
* Correspondence: zhangbaoyun0105@163.com (B.Z.); gqiuli@mail.cgs.gov.cn (Q.G.)

Abstract: To investigate the influence of the Hutuo River (North China) ecological water replenishment project on the hydrogeochemical processes of groundwater, 64 groundwater samples collected at different time intervals after four replenishment events, and four samples from the Middle Route of the South-to-North Water Diversion Project water, were analyzed for water chemistry. Hydrogeochemical methods such as the Piper diagram, chloride-alkalinity index, and ion correlation were employed to analyze the characteristics of groundwater chemical evolution through replenishment. The results demonstrated that the hydrochemical types of groundwater in the study area underwent significant changes during continuous replenishment in the Hutuo River region. During the initial replenishment period (October 2019), the dominant hydrochemical type of groundwater in the study area was Mg-Na-HCO_3-SO_4, whereas the dominant type in the Middle Route of the South-to-North Water Diversion Project water was Ca-Na-SO_4-HCO_3. As the replenishment continued, the hydrochemical types of groundwater in the study area evolved into Ca-Na-Mg-HCO_3-SO_4, Na-Ca-Mg-HCO_3-SO_4, and Ca-Na-Mg-SO_4-HCO_3. The groundwater experienced a dissolution of calcite, gypsum, nitratine, carbonate rocks, and gypsum, accompanied by dilution effects, resulting in reduced ion exchange as replenishment progressed. The input of the high quality Middle Route of South-to-North Water Diversion Project water effectively promoted groundwater quality improvement, leading to an overall decrease or stabilization of components other than Ca^{2+} in the groundwater. Water quality was assessed using the entropy water quality index, with indicators including Na^+, SO_4^{2-}, Cl^-, pH, total dissolved solids, NO_3^--N, NO_2^--N, F^-, Al, As, and Zn. The evaluation results showed that, except for one medium-quality water sample, the water quality of the other samples was suitable for drinking and domestic purposes during the early replenishment period. The Middle Route of the South-to-North Water Diversion Project exhibited excellent quality (Rank 1), and as replenishment progressed, all water samples demonstrated good quality by October 2020, with a gradual improvement.

Keywords: groundwater replenishment; hydrogeochemistry; water-rock interaction; entropy water quality index; Hutuo River

Citation: Zhang, R.; Zhang, B.; Guo, Y.; Kong, X.; Li, Y.; Liu, Y.; Chen, L.; Gong, Q. Replenishment Impacts on Hydrogeochemistry and Water Quality in the Hutuo River Plain. *Water* **2023**, *15*, 3326. https://doi.org/10.3390/w15193326

Academic Editors: Qiting Zuo, Dunxian She, Zengliang Luo, Xiuyu Zhang, Fuqiang Wang, Jiaqi Zhai, Lei Zou and Rong Gan

Received: 23 August 2023
Revised: 13 September 2023
Accepted: 20 September 2023
Published: 22 September 2023

1. Introduction

Owing to the increasing demand for water resources by humans, the balance between groundwater extraction and replenishment has been disrupted, and excessive groundwater exploitation has become a global challenge [1]. Overexploitation of groundwater has led to significant changes in the ecological environment, including river depletion and deterioration of water quality [2–4]. Groundwater replenishment is an effective measure

to alleviate water scarcity and improve the water environment. River infiltration, which replenishes surface water into aquifers, is a fast and efficient method of groundwater replenishment [5–7].

During the ecological replenishment process, replenished water and groundwater interact [8], leading to hydrogeochemical changes in the groundwater and specific reactions with the aquifer medium [9,10]. Daesslé et al. [11] found that, in a groundwater replenishment process in Mexico, wastewater replenishment disrupted the acid-base balance of groundwater and altered the direction of carbonate dissolution and precipitation. Bartak [12] and Kurki [13] investigated groundwater replenishment in India, Finland, and other locations and discovered that river infiltration replenishment gradually impacted the lithology of the aquifer. Greskowiak [14] found that during the process of artificial groundwater replenishment, the change in redox conditions caused by water replenishment leads to reoxidation of sulfides at the top of the aquifer. Wang et al. [15] found that microbial degradation reduced the concentration of chemical oxidation demand in groundwater during the replenishment process. Su et al. [16] studied the process of Liao River infiltration replenishment and identified stratified reactions and the formation of redox zones at different aquifer depths. During the ecological replenishment period in Ejinaqi, the hydrochemical type remained relatively stable, although the concentrations of major ions increased [17]. In an experiment on replenishing groundwater from south to north through infiltration, researchers discovered that the riverbank filtration could provide turbidity, trace organic substances, and major cations and anions in the Yongding River [18].

The replenishment of water into the underground aquifer causes changes in the temperature and oxidative environment of the aquifer, leading to changes in ion concentrations in groundwater [19,20]. Water, as a carrier of pollutants, can induce 70% of diseases, and 20% of cancer cases worldwide are related to water pollution [21,22]. Long-term consumption of contaminated water with nitrates can lead to "blue baby syndrome" disease in infants [23,24]. Prolonged consumption of contaminated water with fluoride levels exceeding the standard limits can cause dental and skeletal fluorosis [25–27]. Shen et al. [28] (2010) found a linear relationship between fluoride concentration and the prevalence of dental fluorosis. Li et al. [29,30] concluded that a study on groundwater quality and health risk assessment is necessary.

The alluvial fan of the Hutuo River in the North China Plain is an important economic development zone; however, it is plagued by ecological problems such as river drying and groundwater funneling [31], which has garnered significant attention from hydrogeologists [32]. To improve this situation, with the completion of the central part of the Middle Route of the South-to-North Water Diversion Project, water diversion has become a new method to alleviate water shortages in North China. The diversion of water in the Middle Route of the South-to-North Water Diversion Project will inevitably cause changes in the hydrochemical characteristics and water quality of the groundwater. Chemical characterization is the basis for studying the chemical composition and evolution of groundwater [33,34]. Previous studies have extensively explored the water-rock interaction mechanisms [35,36], water quality assessment, and prediction [37,38] during the continuous excessive exploitation of groundwater in this region. However, the hydrochemical evolution characteristics and water quality during the groundwater replenishment process are still unclear. This study will help to ensure the water quality safety of replenishment areas, as well as avoid and prevent pollution risks during the groundwater replenishment process.

2. Study Area

The Hutuo River is located in the North China Plain. The study area is located in the middle zone of the Hutuo River from Xinhua district in Shijiazhuang City to Gaocheng district in the east and is the main receiving area of the Hutuo River in the central part of the Middle Route of the South-to-North Water Diversion Project, with a length of approximately 40 km (Figure 1). This region mainly has a temperate, semihumid, and semiarid continental

monsoon climate. Over the years, the average temperature in the study area has been 13.9 °C. The study area has the characteristic of simultaneous rainfall and heat [39], with precipitation mainly concentrated from June to August, accounting for about 80% of the annual precipitation [40]. The average annual precipitation is 484.0 mm.

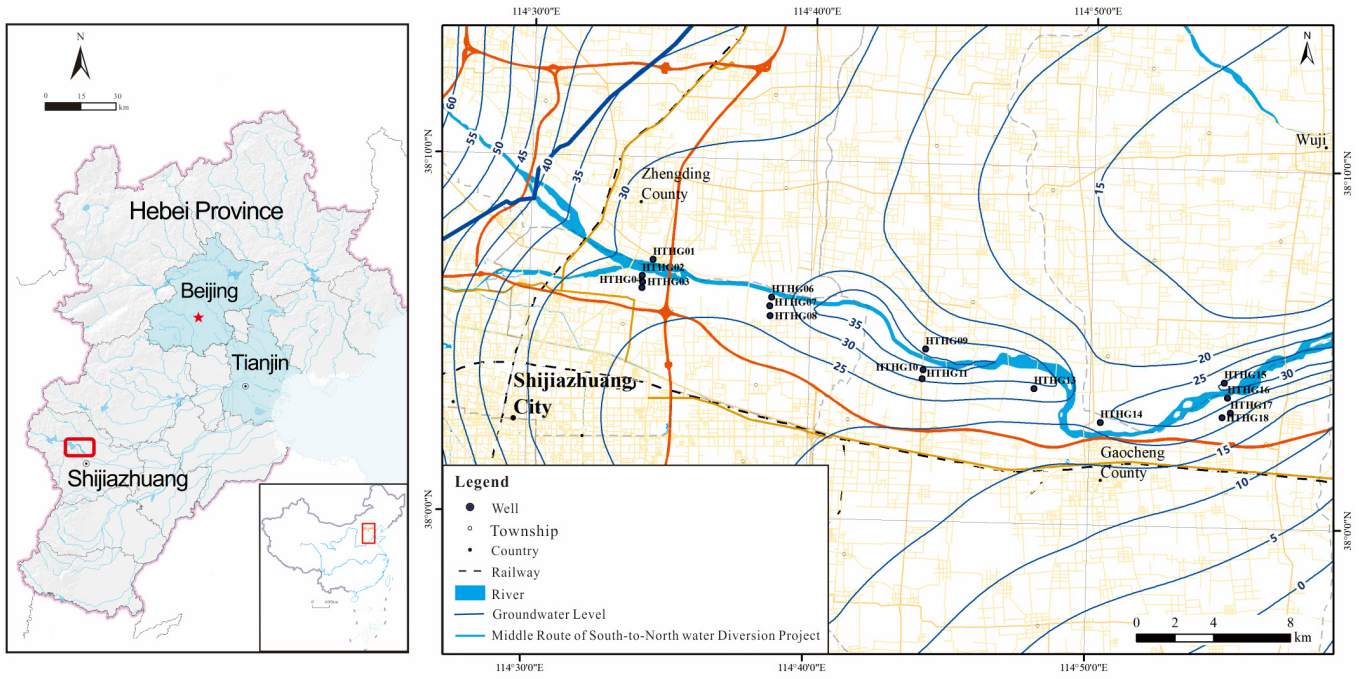

Figure 1. Location of the study area.

The study area is located in the southwest of the Jizhong Depression Belt. Groundwater mainly exists in the pores of sand and gravel layers in the Quaternary system. The aquifer is a complex hydrogeological medium composed of various types of formations, which are typical of porous aquifers. In the vertical direction, the upper and lower sand layers of the aquifer have finer grain sizes and smaller thicknesses. For the middle sand layer, the grain size is coarser and the thickness is larger. The distribution pattern of aquitards is that the upper-middle part mostly consists of discontinuous weak aquitards, and the lower part is mainly composed of cohesive soil aquitards. The aquifer is primarily composed of medium-to-fine sand owing to fluvial and lacustrine deposition and is arranged in a northeast direction (Figure 2). Based on the testing results of the borehole core and previous research findings, the minerals in the aquifer include nitratine, halite, gypsum, calcite, and dolomite [41–44]. Since the 1980s, as the groundwater extraction in the region increased, the groundwater table has gradually deepened, resulting in local drawdown cones [45,46]. Currently, the shallow groundwater in the first aquifer group is largely dewatered, and the second aquifer group is mainly used for industrial, agricultural, and domestic water supplies, with groundwater levels generally at depths of 35–50 m. The aquifer has good permeability and water abundance, with individual good yields ranging from 1000 to 2000 m^3/d. The main sources of groundwater recharge include atmospheric precipitation, lateral runoff, river infiltration, and irrigation return flows. Groundwater discharge occurs mainly through artificial pumping, whereas only a small portion occurs through groundwater evaporation and lateral runoff.

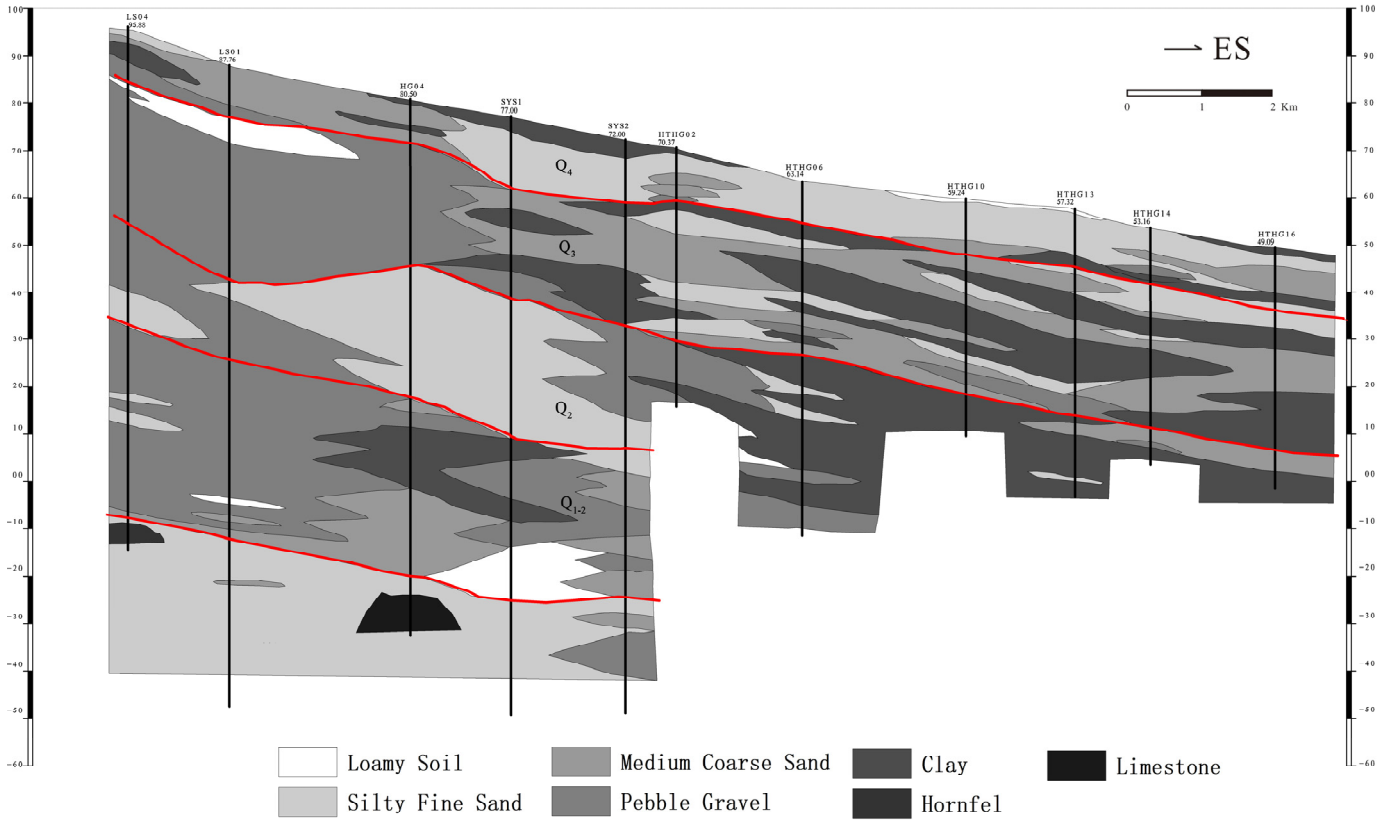

Figure 2. Diagram of hydrogeological profile.

The Shijiazhuang outlet of the Middle Route of the South-to-North Water Diversion Project has been continuously releasing water into the rivers since September 2018. From September 2018 to October 2021, the monthly average water replenishment volume was 0.4×10^8 m^3. The largest replenishment volume was observed in November 2018, with a total of 2.66×10^8 m^3 released into the river in October and November. A minimum volume of 0.05×10^8 m^3 was released in February 2020. For the remaining months, the water replenishment volume remained between 0.13×10^8 and 0.64×10^8 m^3/month. According to the groundwater dynamic monitoring points installed on both sides of the river, it was observed that the groundwater levels on both sides of the river rose due to ecological replenishment caused by the Middle Route of the South-to-North Water Diversion Project. In 2019, the observed impact range of the rising water level on one side of the river was 10 km, in 2020 it was 18 km, and in 2021 it was 23 km.

3. Materials and Methods

3.1. Water Sample Collection and Analysis

This study involved construction of 16 new underground groundwater monitoring wells along the Hutuo River, which flows from the sluice gate of the South-North Water Diversion (Figure 1). The wells have a depth of 45–50 m and are distributed within a 2 km range along the riverbank. During the pilot period of the Hutuo River water replenishment from 2019 to 2021, 64 sets of groundwater samples and 4 sets of surface water samples were collected on four separate occasions. The length of the screen pipe for sampling wells in the study area was 1–10 m. The distance from the bottom of the screen pipe to the bottom of the well was 10–20 m. Firstly, water was pumped to clean the monitoring well, and then on-site testing and sample collection were conducted. Portable multifunctional water quality testers were used for on-site testing of total dissolved solids (TDS) and pH. The data were recorded when the measured values were stable. Polyethylene sampling bottles were used for collecting samples. They were first rinsed with ultrapure water and then

flushed with water samples three times. The water samples were collected in two bottles. One sample of 1.5 L was collected for routine analysis of anions and cations. The other sample of 500 mL was collected for trace element detection when 1:1 HNO_3 was added until pH < 2.

Sample analysis was divided into on-site determination and laboratory determination. For on-site testing, the HCO_3^- and CO_3^{2-} were analyzed using the titration method. The HCO_3^- concentration was determined using the methyl orange endpoint titration method with 0.0048 M H_2SO_4 with a final pH range of 4.2–4.4. The CO_3^{2-} concentration was determined using the phenolphthalein endpoint titration method. Laboratory testing was conducted at the Groundwater Monitoring Center of the Ministry of Natural Resources. K^+, Na^+, Ca^{2+}, Mg^{2+}, Al, and Zn were analyzed using an inductively coupled plasma instrument (ICP-900, Thermo, Waltham, MA, USA). The content of As was detected using an atomic fluorescence spectrometer (AFS-3100, KCHG, Beijing, China). Cl^-, SO_4^{2-}, NO_3^-, NO_2^-, and F^- were analyzed using ion chromatography (ICS-900, Dionex Sunnyvale, CA, USA). The charge balance error for all samples was within 10%.

3.2. Entropy Water Quality Index

In 1965, Horton [47] first proposed a water quality index (WQI). The WQI was calculated using ten commonly used water quality variables, including dissolved oxygen, pH, and alkalinity [48]. Many scholars have applied WQI in their research. Shannon (1948) [49] introduced the concept of entropy, which was integrated by Li et al. (2018) into the traditional WQI, thereby developing the entropy WQI (EWQI) [50].

The weights of the EWQI are more definite and objective than those of previous concepts and have been widely applied in water quality assessment [50]. The calculation steps for EWQI are as follows [51].

$$X = \begin{bmatrix} x_{11} & x_{12} & \cdots & x_{1n} \\ x_{21} & x_{22} & \cdots & x_{2n} \\ \vdots & \vdots & \ddots & \vdots \\ x_{m1} & x_{m2} & \cdots & x_{mn} \end{bmatrix} \quad (1)$$

X_{ij} (i = 1, 2, …, m; j = 1, 2, …, n) represents the initial matrix, where m is the total number of samples, and n is the number of water quality indicators for each sample.

$$y_{ij} = \frac{x_{ij} - (x_{ij})^j_{\min}}{(x_{ij})^j_{\max} - (x_{ij})^j_{\min}} \quad (2)$$

$$Y = \begin{bmatrix} y_{11} & y_{12} & \cdots & y_{1n} \\ y_{21} & y_{22} & \cdots & y_{2n} \\ \vdots & \vdots & \ddots & \vdots \\ y_{m1} & y_{m2} & \cdots & y_{mn} \end{bmatrix} \quad (3)$$

where y_{ij} represents the normalized data value, $(x_{ij})^j_{\max}$ and $(x_{ij})^j_{\min}$ are the minimum and maximum values of indicator j, respectively, and Y is the standardized matrix after normalization.

$$p_{ij} = \frac{y_{ij} + 10^{-4}}{\sum_{i=1}^{m} (y_{ij} + 10^{-4})} \quad (4)$$

$$e_j = -\frac{1}{\ln m} \sum_{i=1}^{m} p_{ij} \ln p_{ij} \quad (5)$$

where e_j represents information entropy and 10^{-4} is the correction factor [52].

$$w_j = \frac{1 - e_j}{\sum_{j=1}^{n} (1 - e_j)} \quad (6)$$

$$q_j = \frac{c_j}{s_j} \times 100 \quad (7)$$

Here, W_j represents the entropy weight and q_j represents the water quality score, c_j is the concentration of the water quality indicator j (mg/L), and s_j is the standard limit value for each indicator (mg/L).

$$EWQI = \sum_{j=1}^{n} w_j \times q_j \quad (8)$$

Li et al. [50] classified the water quality into five levels, ranging from excellent to extremely poor, as listed in Table 1.

Table 1. Classification criteria for groundwater quality based on EWQI.

EWQI	Rank	Water Quality
<25	1	Excellent quality
25–50	2	Good quality
50–100	3	Medium quality
100–150	4	Poor quality
>150	5	Extremely poor quality

4. Results

4.1. Entropy Water Quality Index

Table 2 presents the analysis data of onsite water quality parameters, such as pH, TDS values, and those of the major indicators for groundwater samples. The pH of the groundwater samples was slightly alkaline, with the average pH increasing from 7.25 to 7.94 (October 2019 to October 2021). The maximum value increased from 7.5 to 9.5, and the median value increased from 7.25 to 7.83. The average TDS value of groundwater decreased from 1093.04 to 878.05 mg/L (October 2019 to October 2021), with the maximum value decreasing from 3394.58 to 1694.32 mg/L. The maximum concentration of TDS in October 2019 was 1093.04 mg/L, which decreased to 1694.32 mg/L in October 2020 and then slightly increased to 1972.74 mg/L in October 2021. The same trend was also exhibited by the median value of the TDS.

From October 2019 to October 2021, the concentrations of K^+, Cl^-, and HCO_3^- in the groundwater samples showed small fluctuations. The HCO_3^- concentration varied at a rate of less than 2%, with an average value changing from 325.79 to 346.31 mg/L. Al, As, and Zn were not detected in most of the groundwater samples. The average concentration of Ca^{2+} increased from 42.69 to 125.96 mg/L, with a slight decrease in October 2020 compared to that in April 2020. Except for the aforementioned indicators, the concentrations of the other indicators decreased. From October 2019 to October 2021, the concentration of NO_3^- decreased slightly, with the average value decreasing from 35.51 to 28.52 mg/L. The concentrations of F^- and SO_4^{2-} decreased, with an approximate variation rate of 35%. The concentration of Mg^{2+} decreased significantly, with an average value decreasing from 134.51 to 334.23 mg/L. The decrease in the Mg^{2+} concentration was relative to the injection of water from the Middle Route of the South-to-North Water Diversion Project. Based on the coefficient of variation of each component (Table 2), significant spatial and temporal variability was observed in the dispersion and fluctuation of various ions during the groundwater recharge process. Except for pH, the coefficients of variation for the other components were greater than 0.1, indicating moderate-to-high variability. Among

them, Na^+, Mg^{2+}, Cl^-, NO_3^-, and NO_2^- had variation coefficients greater than one (strong variation), indicating high fluctuations and dispersion at different points, which were possibly influenced by changes in the groundwater environment. The variation coefficients for the other indicators were relatively small, indicating less influence of environmental factors on their concentrations.

A Piper diagram, which is unaffected by subjective human factors, is commonly used to identify the major ion compositions in water chemistry [46]. A Piper diagram (Figure 3) was drawn based on the sampling test data in the study area. According to analysis of the data collected in October 2019, the groundwater type was predominantly Mg-Na-HCO_3-SO_4. The groundwater chemistry type changed to Ca-Na-Mg-HCO_3-SO_4 in April 2020 and to Na-Ca-Mg-HCO_3-SO_4 in October 2020. The chemistry of the Middle Route of the South-to-North Water Diversion Project was primarily Ca-Na-SO_4-HCO_3. As the recharge continued, the predominant chemical type in the area was Ca-Na-Mg-SO_4-HCO_3 in October 2021. The Piper diagram indicates that during the initial stage of recharge, Na^+ and Mg^{2+} were the main groundwater cations, with the highest concentration of Mg^{2+}. As the recharge progressed, the cation concentration decreased in the order of $Ca^{2+} > Na^+ + K^+ > Mg^{2+}$. The main anions were HCO_3^- and SO_4^{2-}. In the early stages of recharge, the groundwater exhibited a chemical characteristic in which strong acid anions were more abundant than weak acid anions. As the recharge progressed, the groundwater chemistry gradually shifted to a characteristic where weak acid anions were greater than those of a strong acid. The characteristics of the anions shifted from mixed and non-carbonate to carbonate types. Based on the above analysis, it can be found that there have been significant changes in ion concentrations in the study area after groundwater recharge. In future research, efforts will be made to enhance the study on hydrogeochemical reactions after groundwater recharge.

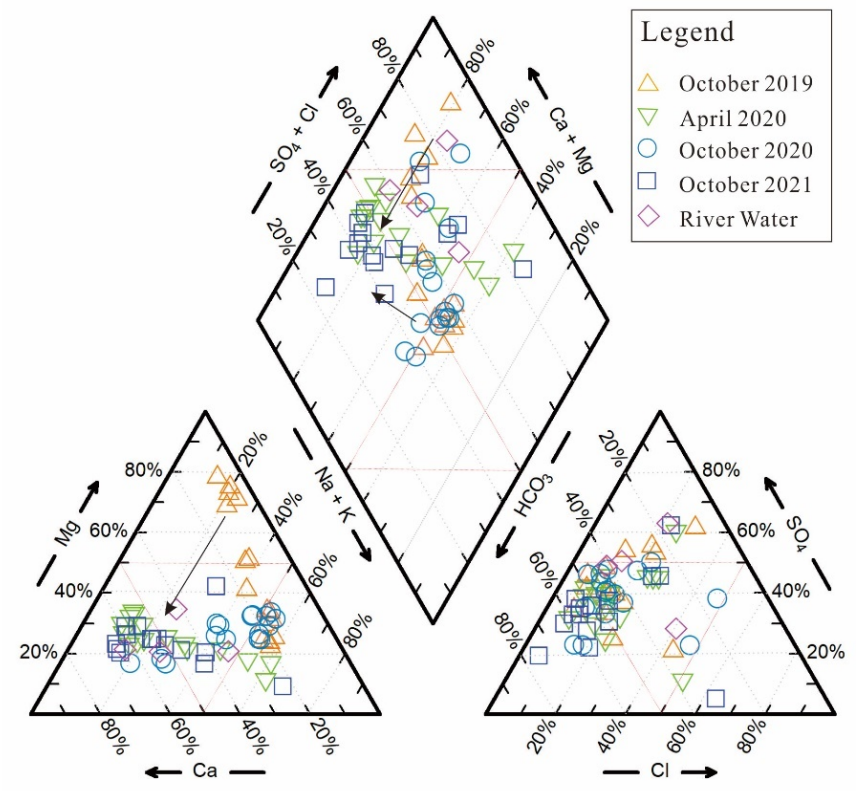

Figure 3. Piper diagram of the study area.

Table 2. Statistics of groundwater hydrochemical components in the researched areas.

Time	Index	K^+	Na^+	Ca^{2+}	Mg^{2+}	Cl^-	$SO_4{}^{2-}$	$HCO_3{}^-$	$NO_3{}^-$	F^-	$NO_2{}^-$	Al	As	Zn	TDS	pH
October 2019	Maximum	7.69	337.6	81.69	689.4	653.6	1863	707.8	149.5	0.65	3.81	ND	ND	ND	3394.58	7.5
	Minimum	1.52	73.64	21.75	26.81	20.26	116.5	245.7	1.65	0.27	ND	ND	ND	ND	510.61	7
	Medium	3.27	135.3	41.08	63.41	71.29	266	344.75	12.49	0.41	0.094	ND	ND	ND	947.91	7.25
	Average	3.84	145.1	42.69	134.51	137.23	378.6	352.79	35.51	0.41	0.43	ND	ND	ND	1093.04	7.25
	Coefficient of Variation	0.45	0.42	0.32	1.22	1.26	1.06	0.31	1.22	0.23	2.15	ND	ND	ND	0.59	0.019
April 2020	Maximum	6.48	545	209	73.1	505	1067	647	147	0.88	0.99	0.048	0.0048	ND	2425	8.2
	Minimum	1.65	24.6	70.8	23.9	18.3	97.9	236	0	0.22	ND	0.012	ND	ND	357	6.7
	Medium	3.17	48.05	134	39.1	75.8	209	331	27.15	0.35	0.0047	0.018	ND	ND	818.5	7.59
	Average	3.39	115.24	133.46	42.55	116.83	269.49	342.63	40.74	0.38	0.088	0.023	0.00044	ND	893.13	7.5
	Coefficient of Variation	0.36	1.15	0.31	0.33	1.05	0.81	0.31	1.05	0.44	2.7	0.43	2.83	ND	0.53	0.049
October 2020	Maximum	6.13	250	383.3	85.69	568.6	620.8	508.3	134.6	0.61	0.073	0.08	ND	ND	1694.32	7.77
	Minimum	1.67	69.25	26.42	23.95	19.6	61.35	213.8	1.44	0.11	ND	ND	ND	ND	402.05	7.04
	Medium	2.4	119.25	48.82	39.68	58.02	214.4	303.35	10.9	0.32	ND	ND	ND	ND	816.86	7.34
	Average	2.69	135.06	100.55	44.52	120.2	257.77	315.975	31.58	0.33	0.0078	0.01	ND	ND	888.18	7.38
	Coefficient of Variation	0.41	0.37	0.97	0.38	1.29	0.55	0.24	1.22	0.48	2.43	2.64	ND	ND	0.37	0.029
October 2021	Maximum	4.85	364.6	234.1	66.83	589.7	824.2	517	88.96	1.59	0.094	0.36	ND	0.13	1972.74	9.5
	Minimum	1.69	8.46	18.03	9	6.83	32.06	129.2	1.6	0	ND	ND	ND	ND	149.37	7.42
	Medium	2.39	43.22	116.2	32.97	47.78	169.6	377.5	11.36	0.15	ND	ND	ND	ND	830.51	7.83
	Average	2.87	93.97	125.96	34.23	119.33	249.82	346.31	28.52	0.26	0.023	0.061	ND	0.018	878.05	7.94
	Coefficient of Variation	0.31	1.07	0.48	0.45	1.28	0.93	0.33	1.03	1.59	1.31	1.81	ND	2.14	0.62	0.061
River Water	Maximum	12.2	81.4	108.4	35.6	114	249	196.8	20.92	0.38	0.079	0.061	ND	ND	507	8.17
	Minimum	4.06	29.84	55.2	20.9	28.75	107	82	1.05	0.19	ND	0.017	ND	ND	148	7.88
	Medium	4.515	48.98	82.33	22.46	51.8	199.35	170.75	8.18	0.32	0.019	0.045	ND	ND	454.5	7.94
	Average	6.32	52.3	82.06	25.35	61.58	188.67	155.07	9.58	0.3	0.029	0.042	ND	ND	391	7.98
	Coefficient of Variation	0.53	52.3	0.25	0.23	0.52	0.28	0.29	0.85	0.25	1.03	0.41	ND	ND	0.37	0.014

Note: ND: not detected.

4.2. Groundwater Quality

According to the standards established by the Chinese Ministry of Health and the National Standardization Management Committee, the acceptable pH range in drinking water is 6.5–8.5. Only the HTHG07 sample collected in October 2021 had a pH value of 9.50, which exceeded the limit. The pH values of other groundwater samples were suitable for drinking. Notably, the pH gradually increased as the recharge progressed. The TDS represents the salinity of water [53]. In October 2019, five groundwater samples had TDS values exceeding the permissible limit for drinking water (1000 mg/L), with the maximum TDS value at the HTHG18 site reaching 3394.58 mg/L and an average value of 1093.04 mg/L. As the recharge continued, the mixing and dilution effects decreased the average TDS value. Two groundwater samples of April 2020 had TDS values that exceeded the permissible limit for drinking water, with the maximum TDS value at the HTHG18 site falling to 2425.21 mg/L. Five groundwater samples collected in October 2020 and four collected in October 2021 exhibited values exceeding the limit; however, the number of samples exceeding the limit decreased. The smaller number of samples collected in April 2020 may be related to seasonal variations. The pH and TDS values of water from the Middle Route of the South-to-North Water Diversion Project did not exceed the limits and were suitable for drinking.

Na^+, SO_4^{2-}, and Cl^- are common indicators of water quality that do not pose health issues (World Health Organization, 2011). However, these ions may influence the drinking water's taste and can be used as indicators of anthropogenic water pollution [54]. The Chinese Drinking Water Quality Standard sets acceptable limits for Na^+ at 200 mg/L and for both SO_4^{2-} and Cl^- at 250 mg/L. In this study, the highest exceedance of the acceptable limit was observed for the SO_4^{2-} concentration. Nine groundwater samples collected in October 2019 exceeded the permissible limit, whereas this limit was exceeded by only three groundwater samples in October 2021. As the recharge progressed, the groundwater quality improved, with the maximum concentration of SO_4^{2-} ions decreasing from 1863 to 620.8 mg/L. Several individual groundwater samples exceeded the limits for Na^+ and Cl^-. Two samples exceeded the limit for the Na^+ concentration, while those exceeding the limit for the Cl^- concentration decreased from two in October 2019 to only one in October 2021. As the recharge continued, the concentrations of Na^+ and Cl^- decreased, which improved the drinking water's taste. The Na^+, SO_4^{2-}, and Cl^- indicators in water from the Middle Route of the South-to-North Water Diversion Project were significantly lower than the permissible limits and were suitable for drinking.

Nitrogen and its compounds are significant in agricultural production [55], and the nitrate concentration is commonly used as an indicator of non-point source pollution in agricultural areas [56]. Based on the Chinese Groundwater Quality Standard, the maximum permissible limits for NO_3^--N and NO_2^--N are 10 and 1 mg/L, respectively. In this study, only one groundwater sample collected in October 2019 (HTHG08) exceeded the permissible limit for the NO_2^--N concentration, whereas the NO_2^--N concentrations in other groundwater samples, including those from the Middle Route of the South-to-North Water Diversion Project, were suitable for drinking. Nitrate (NO_3^--N) showed a relatively severe exceedance, with five samples collected in October 2019 exceeding the limit, with a maximum value of 33.76 mg/L. As the recharge progressed, the NO_3^--N concentration decreased, with three samples collected in October 2021 exceeding the limit. The maximum value decreased to 20.09 mg/L. F^- is beneficial for human health at low concentrations [57,58] but toxic at high levels [59]. Ideally, the concentration of F^- in drinking water should be between 0.5 and 1.0 mg/L [53]. The F^- values of the groundwater samples in the study areas were within an acceptable range for drinking water (<1 mg/L). As is toxic to human health and a well-known carcinogen [60]. The maximum permissible limit of As in drinking water is 0.01 mg/L, and none of the samples in the study areas exceeded this limit. The concentrations of Al and Zn in all the water samples were low and below the limits acceptable for drinking water.

5. Discussion

In hydrogeochemical processes, water-rock interaction is the most significant factor [61], and hydrogeochemical data are vital in studying the evolution of hydrogeochemical processes [62]. During the recharge of external water, groundwater is mainly influenced by the water-rock interactions and mixing-dilution processes [63]. Through hydrogeochemical investigations of groundwater, the formation mechanisms and evolutionary processes of groundwater chemical characteristics can be elucidated.

5.1. Hydrogeochemical Processes

The correlation between anions and cations and the variation in correlation coefficients can be used to infer geochemical processes such as water-rock interactions [64]. Based on the testing results of the borehole core and previous research findings, the minerals in the aquifer include nitratine, halite, gypsum, calcite, and dolomite [41–44]. The proportional relationships of the major ions were plotted (Figure 4), and the correlation coefficients between the different ions for each group of water samples were obtained. The scatter plot of Mg^{2+} and HCO_3^- (Figure 4a) shows a strong correlation in the water samples from April 2020, October 2020, October 2021, and the Middle Route of the South-to-North Water Diversion Project, indicating a possible dissolution of dolomite. The scatter plot of Na^+ and Cl^- (Figure 4b) also revealed a strong correlation, suggesting that the main source of these ions was rock salt dissolution. Theoretically, the ratio of Na^+ to Cl^- should be 1:1; however, most of the groundwater sampling points in these areas fall below the y = x line. This means that the Na^+ concentration in the groundwater samples was higher than the Cl^- concentration, possibly because of the exchange of Na+ adsorbed in the rock layers with Ca^{2+} and Mg^{2+} in the water. There is a good correlation between Na^+ and SO_4^{2-}, except for slightly weaker correlation in the data from October 2020 (R = 0.61) (Figure 4c). The dissolution of nitratine may influence the distribution of chemical elements in the groundwater. If ions are only controlled by the dissolution of gypsum and carbonate rocks, the ratio of (SO_4^{2-} + HCO_3^-) to (Ca^{2+} + Mg^{2+}) should be equal [65]. The proportional relationship between (SO_4^{2-} + HCO_3^-) and (Ca^{2+} + Mg^{2+}) should be on the 1:1 line in the scatter plot, where the y = x line represents the dissolution line of carbonate rocks and gypsum (Figure 4d). Almost all water samples in the graph fall into the region with relatively higher (SO_4^{2-} + HCO_3^-) content. This suggests that the area underwent substantial cation exchange after the dissolution of carbonate rocks and gypsum, where dissolved Ca^{2+} and Mg^{2+} were exchanged with Na^+ adsorbed in the aquifer.

Ratio plots were used to further investigate the origin of ions and the main hydrogeochemical processes. The chloro-alkaline index (CAI) is used to characterize ion exchange processes and the strength of the ion exchange during groundwater chemical evolution [66], which can be expressed as (9) and (10). The range of CAI-1 values for groundwater samples in the study areas was −7.92–0.42, with an average of −1.45. The CAI-2 values ranged from −0.72 to 0.28, with an average of −0.22. During the initial recharge stage, most groundwater samples had negative values for CAI-1 and CAI-2 (Figure 5a), indicating a reverse cation exchange, where Ca^{2+} and Mg^{2+} in the groundwater exchanged with Na^+ in the surrounding rock. In the continued recharging process, the CAI-1 and CAI-2 values tended to become positive, indicating forward cation exchange. Groundwater samples with positive CAI-1 and CAI-2 values were obtained primarily in October 2020 and October 2021. In terms of the magnitudes of the two indices, the absolute values were larger in the early recharge stage, indicating stronger ion exchange. As the recharge progressed, the absolute values decreased, indicating a lower ion exchange intensity compared with that in the early recharge stage. In the plot of (Ca^{2+} + Mg^{2+}) and SO_4^{2-}, samples close to the 1:1 balance line indicate that Ca^{2+} and Mg^{2+} in groundwater are primarily derived from sulfate dissolution [67]. Most groundwater samples were distributed above the 1:1 line (Figure 5b), indicating short-term dilution after the recharge of the Middle Route of the South-to-North Water Diversion Project. In addition to the effects of cation exchange, salt leaching and filtration in the groundwater increased. Gibbs [68] categorized the chemical effects of

groundwater into three types: evaporation-controlled, water-rock interaction-controlled, and precipitation-controlled. The Gibbs diagram is used to study the sources of hydrochemical components and analyze the formation mechanism of hydrochemistry [69]. A Gibbs diagram of the study areas was plotted (Figure 5d), and the main factors controlling the groundwater hydrochemical components were analyzed. Most points fell within the region controlled by water-rock interactions, with only a few pre-recharge samples located in the evaporation-controlled region. The formation of regional hydrochemical types is mainly controlled by water-rock interactions, with a minor influence of evaporation on the hydrochemical categories of water.

$$\mathrm{CAI}-1=\frac{\mathrm{Cl}^{-}-\left(\mathrm{Na}^{+}+\mathrm{K}^{+}\right)}{\mathrm{Cl}^{-}} \tag{9}$$

$$\mathrm{CAI}-2=\frac{\mathrm{Cl}^{-}-\left(\mathrm{Na}^{+}+\mathrm{K}^{+}\right)}{\left(\mathrm{SO}_4^{2-}+\mathrm{HCO}_3^{-}+\mathrm{CO}_3^{2-}+\mathrm{NO}_3^{-}\right)} \tag{10}$$

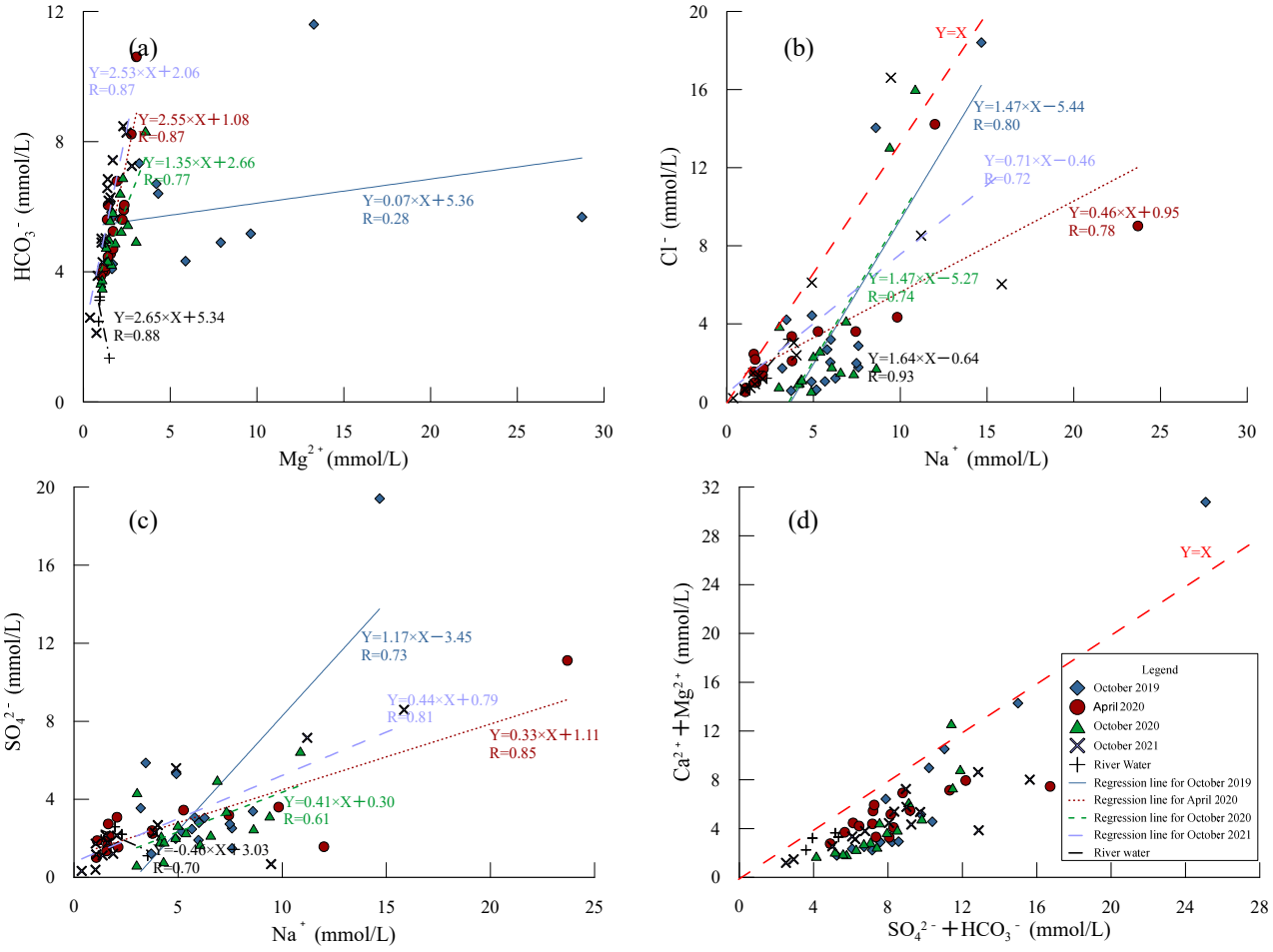

Figure 4. Scatter plots showing the ratio relationships between anions and cations in groundwater.

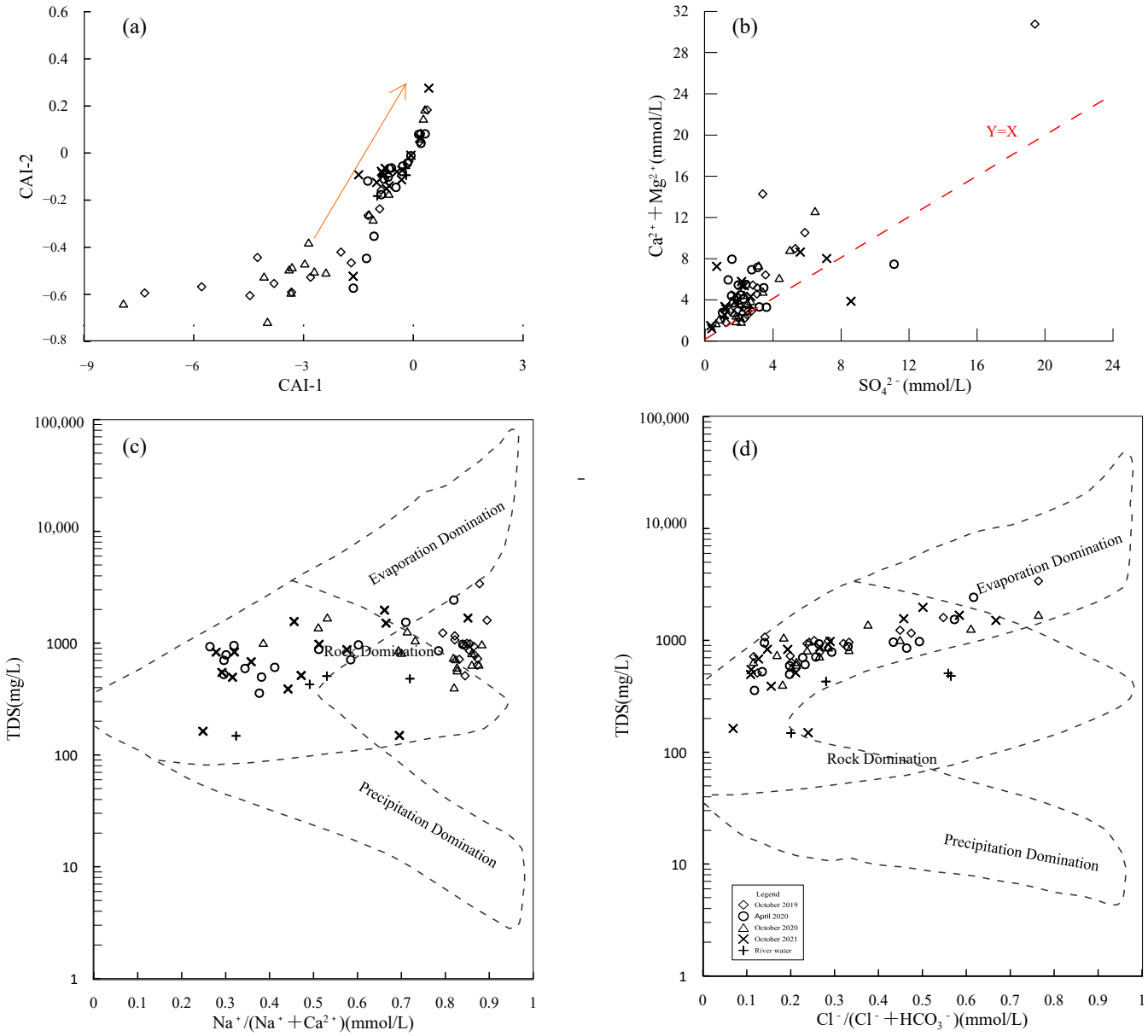

Figure 5. Graphs showing hydrochemical characteristic indicators. (**a**) Relationship between CAI-1 and CAI-2. (**b**) Relationship between SO_4^{2-} and Ca^{2+} + Mg^{2+}. (**c**) The relationship between $Na^+/(Na^+ + Ca^{2+})$ and TDS. (**d**) The relationship between $Cl^-/(Cl^- + HCO_3^-)$ and TDS.

5.2. Changes in Groundwater Quality during the Recharge Process

In this study, water quality parameters such as Na^+, SO_4^{2-}, Cl^-, pH, TDS, NO_3^--N, NO_2^--N, F^-, Al, As, and Zn were selected for overall water quality assessment using the EWQI. The calculated EWQI results are listed in Table 3.

In October 2019, the EWQI values of the groundwater ranged from 13.12 to 84.18. Eleven groundwater samples were classified as excellent quality water samples (Rank 1) and four samples were classified as good quality water samples (Rank 2), indicating that they could be used for various purposes without treatment [70]. One sample (HTHG18) was classified as medium quality water (Rank 3) and could be used for drinking after a preliminary treatment. In April 2020, the EWQI of the groundwater samples ranged from 5.84 to 53.85. Ten groundwater samples were classified as excellent quality water (Rank 1), five samples were classified as good quality water (Rank 2), and one sample (HTHG18) was classified as medium quality water (Rank 3). As the recharge progressed,

the water quality also changed. In October 2020, the EWQI values of the groundwater samples ranged from 11 to 40.4, with 11 high quality water samples (Rank 1) and five good quality water samples (Rank 2). In October 2021, the EWQI values of groundwater samples ranged from 7.51 to 48.12, and the water quality classification was the same as that of the samples collected in October 2020. The EWQI values of the Middle Route of the South-to-North Water Diversion Project ranged from 5.4 to 22.71, and all samples were classified as excellent quality water (Rank 1). The average EWQI value for October 2019 was 26.42, and as the recharge progressed, the average EWQI value for samples collected in October 2021 decreased to 22.02.

Table 3. EWQI values of groundwater samples.

Time	October 2019			April 2020			October 2020			October 2021		
ID	**EWQI**	**Rank**	**Water Quality**	**EWQI**	**Rank**	**Water Quality**	**EWQI**	**Rank**	**Water Quality**	**EWQI**	**Rank**	**Water Quality**
HTHG01	30.41	2	Good quality	24.69	1	Excellent quality	20.35	1	Excellent quality	19.04	1	Excellent quality
HTHG02	17.87	1	Excellent quality	19.56	1	Excellent quality	14.31	1	Excellent quality	16.88	1	Excellent quality
HTHG03	13.12	1	Excellent quality	9.34	1	Excellent quality	19.12	1	Excellent quality	9.95	1	Excellent quality
HTHG04	16.58	1	Excellent quality	12.17	1	Excellent quality	21.45	1	Excellent quality	8.48	1	Excellent quality
HTHG06	13.71	1	Excellent quality	9.50	1	Excellent quality	13.31	1	Excellent quality	26.30	2	Good quality
HTHG07	9.14	1	Excellent quality	5.84	1	Excellent quality	11.01	1	Excellent quality	7.51	1	Excellent quality
HTHG08	48.87	2	Good quality	46.90	2	Good quality	29.45	2	Good quality	11.99	1	Excellent quality
HTHG09	33.2	2	Good quality	29.71	1	Excellent quality	25.79	2	Good quality	46.66	2	Good quality
HTHG10	17.15	1	Excellent quality	10.85	1	Excellent quality	22.45	1	Excellent quality	14.39	1	Excellent quality
HTHG11	18.69	1	Excellent quality	21.74	1	Excellent quality	14.53	1	Excellent quality	17.09	1	Excellent quality
HTHG13	23.03	1	Excellent quality	26.07	2	Good quality	30.40	2	Good quality	12.70	1	Excellent quality
HTHG14	31.51	2	Good quality	39.59	2	Good quality	33.22	2	Good quality	21.60	1	Excellent quality
HTHG15	24.25	1	Excellent quality	17.79	1	Excellent quality	23.86	1	Excellent quality	20.16	1	Excellent quality
HTHG16	23.84	1	Excellent quality	17.59	1	Excellent quality	19.97	1	Excellent quality	40.35	2	Good quality
HTHG17	17.22	1	Excellent quality	27.30	1	Excellent quality	15.65	1	Excellent quality	31.13	2	Good quality
HTHG18	84.18	3	Medium quality	53.85	3	Medium quality	40.41	2	Good quality	48.12	2	Good quality
River Water	22.71	1	Excellent quality	19.20	1	Excellent quality	5.40	1	Excellent quality	15.25	1	Excellent quality

Overall, the groundwater quality in this region was extremely good. From one medium quality water sample (Rank 3) collected in October 2019 to all samples being of good quality

(Rank 2) or higher in 2021, the groundwater quality has gradually improved. As the recharge progresses, a mixing and dilution effect was observed in the groundwater. The water quality of the Middle Route of the South-to-North Water Diversion Project samples was excellent (Rank 1) and the overall quality of the groundwater was effectively improved with the addition of good quality water.

6. Conclusions

This study used monitoring data of recharged groundwater in the Hutuo River area to explore the impacts of groundwater recharge on hydrogeochemistry and water quality in the region. The main conclusions are as follows:

(1) Overall, the groundwater in the area was slightly alkaline, and the pH increased as the recharge progressed. The TDS in the groundwater tended to be high but gradually decreased with recharge. The concentration of Ca^{2+} increased, whereas that of other elemental ions typically decreased or stabilized. Elemental concentrations in sample of the Middle Route of the South-to-North Water Diversion Project were generally lower than those in the groundwater.

(2) Significant changes were observed in the chemical composition of groundwater during concentrated and continuous recharge processes in the Hutuo River area. In the early stages of recharge (October 2019), the groundwater in the study area was mainly of the type Mg-Na-HCO_3-SO_4, while the water from the Middle Route of the South-to-North Water Diversion Project was mainly of the type Ca-Na-SO_4-HCO_3. As the recharge continued, the groundwater in the study area evolved into Ca-Na-Mg-HCO_3-SO_4, Na-Ca-Mg-HCO_3-SO_4, and Ca-Na-Mg-SO_4-HCO_3. Groundwater primarily undergoes the dissolution of minerals, such as calcite, halite, mirabilite, carbonate rocks, and gypsum, accompanied by a dilution effect, and the intensity of ion interactions decreases as the recharge progresses.

(3) The water quality was evaluated using the EWQI. The evaluation results indicated that in the early stages of recharge (October 2019), except for one medium quality water sample, the other water samples exhibited good quality and were suitable for drinking and domestic use. In April 2020, one fair quality sample persisted; however, the overall EWQI value decreased. The water from the Middle Route of the South-to-North Water Diversion Project was of excellent quality (Rank 1), and as the recharge progressed, by October 2020, all water samples exhibited good quality, indicating a gradual improvement in water quality.

Author Contributions: R.Z. and B.Z. conceptualized the core idea, and wrote the initial draft of the paper. Y.G. and Y.L. (Yasong Li) analyzed the data, supervised the research and finalized this paper. X.K. and Y.L. (Yaci Liu) carried out additional analyses and editing of the early version of the manuscript. L.C. and Q.G. contributed to the writing and revisions. All authors have read and agreed to the published version of the manuscript.

Funding: The research was supported by National Natural Science Foundation of China, Grant/Award Number: 41907175, the National Water Pollution Control and Treatment Science and Technology Major Project (No. 2018ZX07109-004), with contributions by the China Geological Survey project, Grant/Award Number DD201903034, the Fundamental Research Funds of Chinese Academy of Geological Sciences (YK202303), and Fundamental Research Funds of Chinese Academy of Geological Sciences (CAGS) (SK202113).

Data Availability Statement: This manuscript does not contain associated data.

Acknowledgments: Peiyue Li and Yuchen Zhu are acknowledged for their assistance and guidance.

Conflicts of Interest: The authors declare no conflict of interest.

References

1. Regnery, J.; Li, D.; Lee, J.; Smits, K.M.; Sharp, J.O. Hydrogeochemical and microbiological effects of simulated recharge and drying within a 2D meso-scale aquifer. *Chemosphere* **2020**, *241*, 125116. [CrossRef] [PubMed]

2. Zhang, Z.; Xu, Y.; Zhang, Y.; Guo, L.; Wang, Z.; Zheng, Q. Impact of groundwater overexploitation on karst aquifer and delineation of the critical zones: Case study of Jinci spring in Shanxi, China. *Carbonates Evaporites* **2022**, *37*, 68. [CrossRef]
3. Dhaouadi, L.; Besser, H.; Karbout, N.; Wassar, F.; Alomrane, A.R. Assessment of natural resources in tunisian Oases: Degradation of irrigation water quality and continued overexploitation of groundwater. *Euro-Mediterr. J. Environ. Integr.* **2021**, *6*, 36. [CrossRef]
4. Zhang, B.; Chen, L.; Li, Y.; Liu, Y.; Li, C.; Kong, X.; Zhang, Y. Impacts of River Bank Filtration on Groundwater Hydrogeochemistry in the Upper of Hutuo River Alluvial Plain, North China. *Water* **2023**, *15*, 1343. [CrossRef]
5. Dillon, P.; Stuyfzand, P.; Grischek, T.; Lluria, M.; Pyne, R.; Jain, R.C.; Bear, J.; Schwarz, J.; Wang, W.; Fernandez, E.; et al. Sixty years of global progress in managed aquifer recharge. *Hydrogeol. J.* **2019**, *27*, 1–30. [CrossRef]
6. Igwebuisi, N.; Muchingami, I.; Kangerere, T. Application of hydrogeophysics and diagnostic plots in setting up a sustainable managed aquifer recharge scheme, West Coast, South Africa. *J. Afr. Earth Sci.* **2023**, *206*, 105039. [CrossRef]
7. Hu, B.; Teng, Y.; Zhai, Y.; Zuo, R.; Li, J.; Chen, H. Riverbank filtration in China: A review and perspective. *J. Hydrol.* **2016**, *541*, 914–927. [CrossRef]
8. Zhang, X.; Zhang, G.; Yan, M. Evolution characteristics of total dissolved solids in the groundwater level funnel area in the Hufu piedmont plain. *Hyd. Eng. Geol.* **2021**, *48*, 72–81. (In Chinese)
9. Hiscock, K.M.; Grischek, T. Attenuation of groundwater pollution by bank filtration. *J. Hydrol.* **2002**, *266*, 139–144. [CrossRef]
10. Bouwer, H. Artificial recharge of groundwater: Hydrogeology and engineering. *Hydrogeol. J.* **2002**, *10*, 121–142. [CrossRef]
11. Daesslé, L.W.; Andrade-Tafoya, P.D.; Lafarga-Moreno, J.; Mahlknecht, J.; Van Geldern, R.; Beramendi-Orosco, L.E.; Barth, J.A.C. Groundwater recharge sites and pollution sources in the wine-producing Guadalupe Valley (Mexico): Restrictions and mixing prior to transfer of reclaimed water from the US-México border. *Sci. Total Environ.* **2020**, *713*, 13. [CrossRef] [PubMed]
12. Bartak, R.; Page, D.; Sandhu, C.; Grischek, T.; Saini, B.; Mehrotra, I.; Jain, C.K.; Ghosh, N.C. Application of risk-based assessment and management to riverbank filtration sites in India Application of risk-based assessment and management to riverbank filtration sites in India. *J. Water Health* **2015**, *13*, 174–189. [CrossRef] [PubMed]
13. Kurki, V.; Lipponen, A.; Katko, T. Managed aquifer recharge in community water supply: The Finnish experience and some international comparisons. *Water Int.* **2013**, *38*, 774–789. [CrossRef]
14. Greskowiak, J.; Prommer, H.; Massmann, G.; Johnston, C.D.; Nützmann, G.; Pekdeger, A. The impact of variably saturated conditions on hydrogeochemical changes during artificial recharge of groundwater. *Appl. Geochem.* **2005**, *20*, 1409–1426. [CrossRef]
15. Wang, C.; Wang, P.F.; Hu, X. Removal of CODcr and nitrogen in severely polluted river water by bank filtration. *Environ. Technol.* **2007**, *28*, 649–657. [CrossRef]
16. Su, D.; Su, X.; Zhang, L.; Yuan, W.; Lu, S.; Zuo, E.; Gao, R. Redox zonation in the process of river water infiltration in the Huangjia riverside well field, Shenyang City. *China Environ. Sci.* **2016**, *36*, 2043–2050.
17. Wang, D.; Yu, J.; Wang, P.; Zhu, B. Shallow Groundwater Chemistry Characteristics and Their Controlling Factors in the Ejina Delta. South-to-North Water Diversion. *Water Sci. Technol.* **2013**, *11*, 51–55. (In Chinese)
18. Zhu, Y.; Zhai, Y.; Teng, Y.; Wang, G.; Du, Q.; Wang, J.; Yang, G. Water supply safety of riverbank filtration wells under the impact of surface water-groundwater interaction: Evidence from long-term field pumping tests. *Sci. Total Environ.* **2020**, *711*, 135141. [CrossRef]
19. Shamrukh, M.; Abdel-Wahab, A. Water Pollution and Riverbank Filtration for Water Supply Along River Nile, Egypt. In *Riverbank Filtration for Water Security in Desert Countries*; Springer: Berlin/Heidelberg, Germany, 2011; pp. 5–28.
20. Boving, T.B.; Patil, K.; D'Souza, F.; Barker, S.F.; McGuinness, S.L.; O'Toole, J.; Sinclair, M.; Forbes, A.B.; Leder, K. Performance of riverbank filtration under hydrogeologic conditions along the upper Krishna river in Southern India. *Water* **2019**, *11*, 17. [CrossRef]
21. Li, P.; Wu, J. Drinking water quality and public health. *Expo. Health* **2019**, *11*, 73–79. [CrossRef]
22. Milovanovic, M. Water quality assessment and determination of pollution sources along the Axios/Vardar River, Southeastern Europe. *Desalination* **2007**, *213*, 159–173. [CrossRef]
23. Mencio, A.; Mas-Pla, J.; Otero, N.; Regas, O.; Boy-Roura, M.; Puig, R.; Bach, J.; Domenech, C.; Zamorano, M.; Brusi, D.; et al. Nitrate pollution of groundwater; all right, but nothing else? *Sci. Total Environ.* **2016**, *539*, 241–251. [CrossRef] [PubMed]
24. Verma, A.; Sharma, A.; Kumar, R.; Sharma, P. Nitrate contamination in groundwater and associated health risk assessment for Indo-Gangetic Plain, India. *Groundw. Sustain. Dev.* **2023**, *23*, 100978. [CrossRef]
25. Ali, S.; Fakhri, Y.; Golbini, M.; Thakur, S.K.; Alinejad, A.; Parseh, I.; Shekhar, S.; Bhattacharya, P. Concentration of fluoride in groundwater of India: A systematic review, meta-analysis and risk assessment. *Groundw. Sustain. Dev.* **2019**, *9*, 100224. [CrossRef]
26. Ali, S.; Shekhar, S.; Bhattacharya, P.; Verma, G.; Gurav, T.; Chandrashekhar, A.K. Elevated fluoride in groundwater of Siwani Block, Western Haryana, India: A potential concern for sustainable water supplies for drinking and irrigation. *Groundw. Sustain. Dev.* **2018**, *7*, 410–420. [CrossRef]
27. Edmunds, W.M.; Smedley, P.L. Fluoride in natural waters. In *Essentials of Medical Geology*; Springer: Dordrecht, The Netherlands, 2012; pp. 311–336.
28. Shen, Z.; Guo, H.; Xu, G.; Wang, C. Abnormal Groundwater Chemistry and Endemic Disease. *Chin. J. Nat.* **2010**, *7*, 83–89. (In Chinese)
29. Li, P.; He, X.; Guo, W. Spatial groundwater quality and potential health risks due to nitrate ingestion through drinking water: A case study in Yan'an city on the loess plateau of northwest China. *Hum. Ecol. Risk Assess.* **2019**, *25*, 11–31. [CrossRef]
30. Li, P.; He, X.; Li, Y.; Xiang, G. Occurrence and health implication of fluoride in groundwater of loess aquifer in the Chinese Loess Plateau: A case study of Tongchuan, Northwest China. *Expo. Health* **2019**, *11*, 95–107. [CrossRef]

31. Li, Y.; Zhang, Z.; Fei, Y.; Chen, H.; Qian, Y.; Dun, Y. Investigation of quality and pollution characteristics of groundwater in the Hutuo River Alluvial Plain, North China Plain. *Environ. Earth Sci.* **2016**, *75*, 581. [CrossRef]
32. Zhang, X.; He, J.; He, B.; Sun, J. Assessment, formation mechanism, and different source contributions of dissolved salt pollution in the shallow groundwater of Hutuo River alluvial-pluvial fan in the North China Plain. *Environ. Sci. Pollut. Res.* **2019**, *26*, 35742–35756. [CrossRef]
33. Massmann, G.; Nogeitzig, A.; Taute, T.; Pekdeger, A. Seasonal and spatial distribution of redox zones during lake bank filtration in Berlin, Germany. *Environ. Geol.* **2007**, *54*, 53–65. [CrossRef]
34. Yuan, J.; Dyke, M.I.V.; Huck, P.M. Water reuse through managed aquifer recharge (MAR): Assessment of regulations/guidelines and case studies. *Water Pollut. Res. J. Can.* **2016**, *51*, 357–376. [CrossRef]
35. Cheng, Z.; Su, C.; Zheng, Z.; Chen, Z.; Wei, W. Characterize groundwater vulnerability to intensive groundwater exploitation using tritium time-series and hydrochemical data in Shijiazhuang, North China Plain. *J. Hydrol.* **2023**, *603*, 126953. [CrossRef]
36. Yuan, R.; Wang, M.; Wang, S.; Song, X. Water transfer imposes hydrochemical impacts on groundwater by altering the interaction of groundwater and surface wate. *J. Hydrol.* **2020**, *583*, 124617. [CrossRef]
37. Fu, J.; Zhang, L.; Liu, Z.; Yu, J. Study on the Sustainable Utilization of Groundwater Resources in Hebei Plain. *Procedia Environ. Sci.* **2021**, *12*, 1071–1076.
38. Ganot, Y.; Holtzman, R.; Weisbrod, N.; Russak, A.; Katz, Y.; Kwtzman, D. Geochemical processes during managed aquifer recharge with desalinated seawater. *Water Resour. Res.* **2018**, *54*, 978–994. [CrossRef]
39. Zhang, Q.; Wang, H.; Wang, L. Tracing nitrate pollution sources and transformations in the over-exploited groundwater region of north China using stable isotopes. *J. Contam. Hydrol.* **2018**, *218*, 1–9. [CrossRef]
40. Zhang, Q.; Wang, H.; Wang, Y.; Yang, M.; Zhu, L. Groundwater quality assessment and pollution source apportionment in an intensely exploited region of northern China. *Environ. Sci. Pollut. Res.* **2017**, *24*, 16639–16650. [CrossRef]
41. Su, X.; Xu, W.; Du, S. Responses of groundwater vulnerability to artificial recharge under extreme weather conditions in Shijiazhuang City, China. *J. Water Supply Res. Technol.* **2014**, *63*, 224–238. [CrossRef]
42. Tian, X.; Meng, S.; Cui, X.; Zhang, X.; Zhang, Z.; Fei, Y. Hydrochemical Effect of Groundwater Recharge in Over-Exploited Area of Hutuo River Basin. *Res. Environ. Sci.* **2021**, *34*, 629–636. (In Chinese)
43. Yan, M.; Wang, Q.; Tian, Y.; Wang, J.; Nie, Z.; Zhang, G. The dynamics and origin of groundwater salinity in the northeast Hufu Plain. *Environ. Earth Sci.* **2016**, *75*, 1154. [CrossRef]
44. Wang, J.; Zhang, C.; Xiong, L.; Song, G.; Liu, F. Changes of antibiotic occurrence and hydrochemistry in groundwater under the influence of the South-to-North Water Diversion (the Hutuo River, China). *Sci. Total Environ.* **2022**, *832*, 154779.
45. Zheng, Y.; Vanderzalm, J.; Hartog, N.; Escalante, E.F.; Stefan, C. The 21st century water quality challenges for managed aquifer recharge: Towards a risk-based regulatory approach. *Hydrogeol. J.* **2022**, *31*, 189. [CrossRef]
46. Piper, A.M. *A Graphic Procedure in the Geochemical Interpretation of Water Analysis*; United States Department of the Interior, Geological Survey, Water Resources Division, Ground Water Branch: Washington, DC, USA; CRC Press: Boca Raton, FL, USA, 1953; p. 63.
47. Horton, R.K. An index number system for rating water quality. *J. Water Pollut. Control Fed.* **1965**, *37*, 300–305.
48. Amiri, V.; Rezaei, M.; Sohrabi, N. Groundwater quality assessment using entropy weighted water quality index (EWQI) in Lenjanat, Iran. *Environ. Earth Sci.* **2014**, *72*, 3479–3490. [CrossRef]
49. Shannon, C.E. A mathematical theory of communication. *Bell Syst. Tech. J.* **1948**, *27*, 379–423. [CrossRef]
50. Li, P.; Wu, J.; Tian, R.; He, S.; He, X.; Xue, C.; Zhang, K. Geochemistry, hydraulic connectivity and quality appraisal of multilayered groundwater in the Hongdunzi Coal Mine, Northwest China. *Mine Water Environ.* **2018**, *37*, 222–237. [CrossRef]
51. Wang, D.; Wu, J.; Wang, Y.; Ji, Y. Finding high-quality groundwater resources to reduce the hydatidosis incidence in the Shiqu County of Sichuan Province, China: Analysis, assessment, and management. *Expo. Health* **2019**, *12*, 307–322. [CrossRef]
52. Tian, R.; Wu, J. Groundwater quality appraisal by improved set pair analysis with game theory weightage and health risk estimation of contaminants for Xuecha drinking water source in a loess area in northwest China. *Hum. Ecol. Risk Assess.* **2019**, *25*, 176–190. [CrossRef]
53. Wu, J.; Zhou, H.; He, S.; Zhang, Y. Comprehensive understanding of groundwater quality for domestic and agricultural purposes in terms of health risks in a coal mine area of the Ordos basin, north of the Chinese Loess Plateau. *Environ. Earth Sci.* **2019**, *78*, 446. [CrossRef]
54. Lin, X.; Yang, A.; Chen, F. Measurement and evaluation of residual disinfection by products in tap water from Xiamen. *IOP Conf. Ser. Earth Environ. Sci.* **2018**, *146*, 012015.
55. Zhang, Y.; Wu, J.; Xu, B. Human health risk assessment of groundwater nitrogen pollution in Jinghui canal irrigation area of the loess region, northwest China. *Environ. Earth Sci.* **2018**, *77*, 273. [CrossRef]
56. Chen, J.; Wu, H.; Qian, H. Groundwater nitrate contamination and associated health risk for the rural communities in an agricultural area of Ningxia, Northwest China. *Expo. Health* **2016**, *8*, 349–359. [CrossRef]
57. Adimalla, N.; Venkatayogi, S. Mechanism of fluoride enrichment in groundwater of hard rock aquifers in Medak, Telangana State, South India. *Environ. Earth Sci.* **2017**, *76*, 45. [CrossRef]
58. Odiyo, J.O.; Makungo, R. Chemical and microbial quality of groundwater in siloam village, implications to human health and sources of contamination. *Int. J. Environ. Res. Public Health* **2018**, *15*, 317. [CrossRef]

59. Fordyce, F.M.; Vrana, K.; Zhovinsky, E.; Povoroznuk, V.; Toth, G.; Hope, B.C.; Iljinsky, U.; Baker, J. A health risk assessment for fluoride in central Europe. *Environ. Geochem. Health* **2007**, *29*, 83–102. [CrossRef]
60. He, X.; Li, P. Surface water pollution in the middle Chinese Loess Plateau with special focus on hexavalent chromium (Cr^{6+}): Occurrence, sources and health risks. *Expo. Health* **2020**, *12*, 385–401. [CrossRef]
61. Duan, R.; Li, P.; Wang, L.; He, X.; Zhang, L. Hydrochemical characteristics, hydrochemical processes and recharge sources of the geothermal systems in Lanzhou City, northwestern China. *Urban Clim.* **2022**, *43*, 101152. [CrossRef]
62. Bekele, E.; Zhang, Y.; Donn, M.; McFarlane, D. Inferring groundwater dynamics in a coastal aquifer near wastewater infiltration ponds and shallow wetlands (Kwinana, Western Australia) using combined hydrochemical, isotopic and statistical approaches. *J. Hydrol.* **2019**, *568*, 1055–1070. [CrossRef]
63. Wang, Z.; Yin, J.; Pu, J.; Wang, P.; Liang, X.; Yang, P.; He, Q.; Gou, P.; Yuan, D. Integrated understanding of the Critical Zone processes in a subtropical karst watershed (Qingmuguan, Southwestern China): Hydrochemical and isotopic constraints. *Sci. Total Environ.* **2020**, *749*, 141257. [CrossRef]
64. Liu, J.; Gao, Z.; Wang, Z.; Xu, X.; Su, Q.; Wang, S.; Qu, W.; Xing, T. Hydrogeochemical processes and suitability assessment of groundwater in the Jiaodong Peninsula, China. *Environ. Monit. Assess.* **2020**, *192*, 17. [CrossRef] [PubMed]
65. Wu, J.; Li, P.; Qian, H.; Duan, Z.; Zhang, X. Using correlation and multivariate statistical analysis to identify hydrogeochemical processes affecting the major ion chemistry of waters: A case study in Laoheba phosphorite mine in Sichuan, China. *Arab. J. Geosci.* **2014**, *7*, 3973–3982. [CrossRef]
66. Guo, X.; Zuo, R.; Wang, J.; Meng, L.; Teng, Y.; Shi, R.; Gao, X.; Ding, F. Hydrogeochemical Evolution of Interaction Between Surface Water and Groundwater Affected by Exploitation. *Groundwater* **2019**, *57*, 430–442. [CrossRef]
67. Han, Y.; Zhai, Y.; Guo, M.; Cao, X.; Lu, H.; Li, J.; Wang, S.; Yue, W. Hydrochemical and isotopic characterization of the impact of water diversion on water in drainage channels, groundwater, and Lake Ulansuhai in China. *Water* **2021**, *13*, 3033. [CrossRef]
68. Gibbs, R.J. Mechanisms controlling world water chemistry. *Science* **1970**, *170*, 1088–1090. [CrossRef] [PubMed]
69. Pant, R.R.; Zhang, F.; Rehman, F.U.; Wang, G.; Ye, M.; Zeng, C.; Tang, H. Spatiotemporal variations of hydrogeochemistry and its controlling factors in the Gandaki River Basin, Central Himalaya Nepal. *Sci. Total Environ.* **2018**, *622–623*, 770–782. [CrossRef]
70. Su, H.; Kang, W.; Xu, Y.; Wang, J. Assessing groundwater quality and health risks of nitrogen pollution in the Shenfu mining area of Shaanxi Province, northwest China. *Expo. Health* **2018**, *10*, 77–97. [CrossRef]